

HBr Formation from the Reaction between Gas-phase Bromine Atom and Vibrationally Excited Chemisorbed Hydrogen Atoms on a Si(001)-(2 × 1) Surface

J. Ree,* S.-H. Yoon, K.-G. Park,[†] and Y. H. Kim[‡]

Department of Chemistry Education, Chonnam National University, Kwangju 500-757, Korea

[†]Ivy Class Student, Korea Minjok Leadership Academy, Hoengsung, Kangwondo 225-823, Korea

[‡]Department of Chemistry and Center for Chemical Dynamics, Inha University, Incheon 402-751, Korea

Received March 15, 2004

We have calculated the probability of HBr formation and energy disposal of the reaction exothermicity in HBr produced from the reaction of gas-phase bromine with highly covered chemisorbed hydrogen atoms on a Si(001)-(2 × 1) surface. The reaction probability is about 0.20 at gas temperature 1500 K and surface temperature 300 K. Raising the initial vibrational state of the adsorbate(H)-surface(Si) bond from the ground to $\nu = 1, 2$ and 3 states causes the vibrational, translational and rotational energies of the product HBr to increase equally. However, the vibrational and translational motions of product HBr share most of the reaction energy. Vibrational population of the HBr molecules produced from the ground state adsorbate-surface bond ($\nu_{\text{HSi}} = 0$) follows the Boltzmann distribution, but it deviates seriously from the Boltzmann distribution when the initial vibrational energy of the adsorbate-surface bond increases. When the vibration of the adsorbate-surface bond is in the ground state, the amount of energy dissipated into the surface is negative, while it becomes positive as ν_{HSi} increases. The energy distributions among the various modes weakly depends on surface temperature in the range of 0-600 K, regardless of the initial vibrational state of H(ad)-Si(s) bond.

Key Words : HBr formation, Bromine, Chemisorbed, Hydrogen, Si

Introduction

In the past several decades, most studies in gas-atom interaction taking place on a solid surface have been performed on highly exothermic reactions. For example, chemisorption energies of atoms such as hydrogen and chlorine on a close-packed metal surface^{1,2} or nonmetallic surface such as graphite and silicon³⁻⁷ lie in the range of 2-3 eV, whereas the energy of the bond formed between the gas and surface atoms is 4-5 eV.⁸ Thus, the reaction exothermicity is about 2 eV, which is to be distributed among various motions of the product, including the solid phase. However, if the chemisorbed atom is hydrogen and the gas-phase atom is bromine, even though it belongs to the same halogen group as chlorine, they don't lead to a highly exothermic reaction but to a slightly endothermic reaction ($\Delta E = 0.008$ eV). Recently, we have studied the reaction of gas-phase bromine atom with highly covered chemisorbed hydrogen atoms on a silicon surface, and reported that the reaction mechanism is the Eley-Rideal type,⁹ even though the reaction is endothermic.

In the same system, however, when the chemisorbed hydrogen atom on a silicon surface is in vibrationally excited states, the reaction can become exothermic. Thus, it should be interesting to study the reaction of gas-phase bromine atom with the vibrationally excited chemisorbed hydrogen atoms on a silicon surface.

In the present paper, we study the reaction of gas-phase

bromine atom with a H-saturated silicon surface with particular emphasis on the disposal of the reaction exothermicity for a range of initial excitation of the adatom-surface vibration. To study the reaction, we will employ a modified version of the London-Eyring-Polanyi-Sato (LEPS) procedure, which includes additional energy terms that result from the participation of adjacent surface sites in the bromine-to-surface interaction,¹⁰ to construct the potential energy surface and use it in the molecular time scale generalized Langevin equation (MTGLE), which is designed to describe the combined motions of reaction-zone atoms and surface atoms.¹¹⁻¹³ Incorporation of surface atom dynamics enables us to determine the flow of energy between the reaction zone and the solid in an accurate way. We consider the reaction that takes place at a gas temperature of 1500K and surface temperature of 300 K. A brief discussion of the dependence of reaction probabilities and product energy distribution on surface temperature will also be presented.

Interaction Model

The interaction model and numerical procedures have been reported already in Ref. 9. We briefly recapitulate the essential aspect of the model for the interaction of atomic bromine with H chemisorbed on the Si(001)-(2 × 1) surface reconstructed by forming dimers along the [110] direction. For easy reference we display the dimer configuration and the collision model in Figure 1 defining the pertinent coordinates. The H atom is chemisorbed on the Si atom of the symmetric dimer structure. This adatom site, which is surrounded by eight adjacent Si atom, is the $N = 0$ member

*Corresponding Author. Tel: +82-62-530-2495; Fax: +82-62-530-2499; e-mail: jbre@chonnam.ac.kr

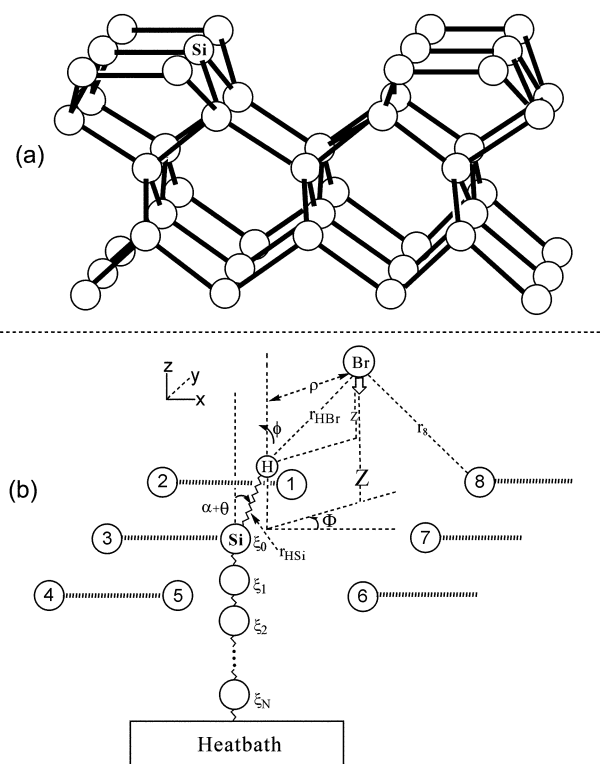


Figure 1. (a) Symmetric Si-Si dimer surface. (b) Interaction model showing the H atom adsorbed on the 0th Si atom, which is coupled to the N -atom chain. The coordinates of the $(N+1)$ chain atoms including the 0th atom are denoted by 0, 1, \dots , N . The 0th atom is identified by Si in both (a) and (b). The N th atom of the chain is coupled to the heat bath. The position of H is defined by $(r_{\text{HSi}}, \theta, \phi)$ and the position of Br by (ρ, Z, Φ) . α is the tilt angle. The Br to H distance is denoted by r_{HBr} , and the Br to the i th surface-layer Si atom distance by r_i .

of the $(N+1)$ -atom chain, which links the reaction zone to the solid heat bath [see Figure 1(b)]. We shall refer to this adatom site as the zeroth Si atom. Thus, in addition to the adatom, the incident atom is in interaction with all these 8+ $(N+1)$ Si atoms, where the zeroth atom on which the hydrogen atom is chemisorbed, is surrounded by eight surface-layer Si atoms and the last chain (N th) atom is bound to the bulk phase. All these interaction energy terms are included in the modified version of the LEPS potential energy surface. Since the gas atom-to-nine surface distances have the functional dependence $r_i \equiv r_i(r_{\text{HSi}}, \theta, \phi, \rho, Z, \Phi)$ and the Br(g)-to-H(ad) distance $r_{\text{HBr}} \equiv r_{\text{HBr}}(r_{\text{HSi}}, \theta, \rho, Z, \Phi)$, we can obtain the potential energy $U(r_{\text{HSi}}, \theta, \phi, \rho, Z, \Phi, \{\xi\})$, where $\{\xi\}$ is the collective notation for $(\xi_0, \xi_1, \dots, \xi_N)$ for the vibrational coordinates of the $(N+1)$ -chain atoms. Here, we have transformed the coordinate of the incident gas atom $(x_{\text{Br}}, y_{\text{Br}}, z_{\text{Br}})$ into the cylindrical system (ρ, Z, Φ) and the adatom coordinate $(x_{\text{H}}, y_{\text{H}}, z_{\text{H}})$ into $(r_{\text{HSi}}, \theta, \phi)$. The adatom is tilted from the surface normal by $\alpha = 20.6^\circ$.¹⁴

For this reaction, the activation energy is known to be only ~ 1.0 kcal/mole.^{15,16} Each Coulomb or exchange term of the LEPS potential function contains the Sato parameter (Δ). By varying their values systematically, we find the Sato

parameters which best describe the desired features of minimizing barrier height and attractive well depth in both the entrance and exit channels to be $\Delta_{\text{HBr}} = 0.30$, $\Delta_{\text{HSi}} = 0.63$ and $\Delta_{\text{BrS}} = 0.37$ for the reaction zone Si atom (*i.e.*, the Br to 0th Si atom) and $\Delta_{\text{BrS}} = 0.37$ for the Br to the remaining eight surface-layer Si atoms.⁹

To study the reactive event, we follow the time evolution of the reaction system by integrating the equations of dynamics, which describe the motions of the reaction-zone atoms and N -chain atoms. An intuitive way to treat the dynamics of the reaction involving many surface atoms is to solve the motions of primary zone atoms governed by the MTGLE set of the equations for the gas atom, adatom, zeroth Si atom and N chain atoms. The equations of motion for the gas atom and adatom are in the form of $m_i \ddot{Y}_i(t) = -U/\partial Y_i$, where $i = 1, 2, \dots, 6$ for $Z, \rho, \Phi, r_{\text{HSi}}, \theta, \phi$, with $m_1 = m_{\text{Br}}$, $m_2 = \mu_{\text{HBr}}$, $m_3 = I_{\text{HBr}}$, $m_4 = \mu_{\text{HSi}}$, $m_5 = m_6 = I_{\text{HSi}}$. Here μ_i and I_i are the reduced mass and the moment of inertia of the interaction system indicated. The potential energy contains the effects of all surface-layer atoms. For the $(N+1)$ -atom chain dynamics, we have⁶

$$M_s \ddot{\xi}_0(t) = -M_s \omega_{e0}^2 \xi_0(t) + M_s \omega_{c1}^2 \xi_1(t) - \partial U(r_{\text{HSi}}, \theta, \phi, \rho, Z, \Phi, \{\xi\}) / \partial \xi_0 \quad (1a)$$

$$M_s \ddot{\xi}_j(t) = -M_s \omega_{ej}^2 \xi_j(t) + M_s \omega_{cj}^2 \xi_{j-1}(t) + M_s \omega_{c,j+1}^2 \xi_{j+1}(t), \quad j = 1, 2, \dots, N-1 \quad (1b)$$

$$M_s \ddot{\xi}_N(t) = -M_s \Omega_N^2 \xi_N(t) + M_s \omega_{c,N}^2 \xi_{N-1}(t) - M_s \beta_{N+1} \dot{\xi}_N(t) + M_s f_{N+1}(t) \quad (1c)$$

In these equations, M_s is the mass of the silicon atom, ω_e the Einstein frequency, ω_c the coupling frequency characterizing the chain, and Ω_N the adiabatic frequency. The friction coefficient β_{N+1} is very close to $\pi\omega_D/6$, where ω_D is the Debye frequency.¹¹ The Debye temperature of Si is 640 K.¹⁷ The quantity $M_s f_{N+1}(t)$ is the random force on the primary system arising from thermal fluctuation in the heat bath. This force balances, on average, the dissipative force, $M_s \beta_{N+1}(t)$, which removes energy from the $(N+1)$ atom chain system in order that the equilibrium distribution of energies in the chain can be restored after collision. The initial conditions needed to solve these equations have already been given in earlier papers.¹⁰

The numerical procedures are given in detail in Ref. 9. We sample 30000 sets for each ensemble. We follow each trajectory for 50 ps, which is a sufficiently long time for HBr(g) to recede from the influence of surface interaction, to confirm the occurrence of a reactive event forming HBr. Furthermore, we confirm that each trajectory can be successfully back-integrated in the computational procedure. We take the chain length of $N=10$.⁶ The pertinent potential and spectroscopic constants^{4,19-24} used in the calculation are listed in Table 1.

Results and Discussion

Since the typical experimental condition for producing bromine atoms is 1500 K,²⁵ we considered the reaction occurring at the gas temperature of 1500 K. At the thermal conditions of $(T_g, T_s) = (1500, 300 \text{ K})$, we find that the probabilities of the $\text{Br}(\text{g}) + \text{H}(\text{ad})/\text{Si} \rightarrow \text{HBr}(\text{g}) + \text{Si}$ reaction for the vibrational state $\nu_{\text{HSi}} = 1, 2$, and 3 are 0.200, 0.202, and 0.221, respectively. The reaction probability at the gas and the surface temperature (T_g, T_s) is defined as the ratio of the number of reactive trajectories N_R to the total number of trajectories $N_T (= 30,000)$ sampled over the entire range of impact parameters. These are very close to the probability for the case in which the HSi vibration is in the ground state, 0.200.⁹ It is interesting to note that reactions for the excited vibrational state of the chemisorbed hydrogen atom ($\nu_{\text{HSi}} = 1, 2$, and 3) are exothermic, whereas the reaction for the ground vibrational state is slightly endothermic ($\Delta E = 0.008 \text{ eV}$). These results are very different from those for the related system of $\text{O}(\text{g})$ interacting with $\text{H}(\text{D})/\text{Si}$, where the probability of OH formation increases linearly with increasing initial excitation of the HSi vibration.²⁶

We first consider the distribution of collision energies for all reactive trajectories in Figure 2 to find the reason why the reaction probability for the HSi vibration in the ground state is as high as those in the excited states, even though the reaction in the ground state is endothermic and the reaction in the excited states is exothermic. For the vibrational state $\nu_{\text{HSi}} = 0$, the reaction is slightly endothermic, and the energy needed for the Si-H dissociation comes in part from the kinetic energy. Thus, Si-H vibration should receive energy from the incident atom (a $\text{T} \rightarrow \text{V}$ pathway) and retain it long enough for the bond to dissociate. We show the distribution of collision energies of reactive trajectories for the vibrational state $\nu_{\text{HSi}} = 0$ in Figure 2(a) with the distribution of total sampled trajectories $N_T (= 30,000)$ (the solid line). Total sampled trajectories, of course, follow the Maxwell distribution with the maximum occurring at $3k_B T/2 = 0.194 \text{ eV}$. However, the collision energy distribution of reactive trajectories for the vibrational state $\nu_{\text{HSi}} = 0$ is skewed to the high-energy shoulder of the Maxwell distribution. Thus, there is an important group of collisions, which can typically be identified as strong collisions. In these collisions Br in the

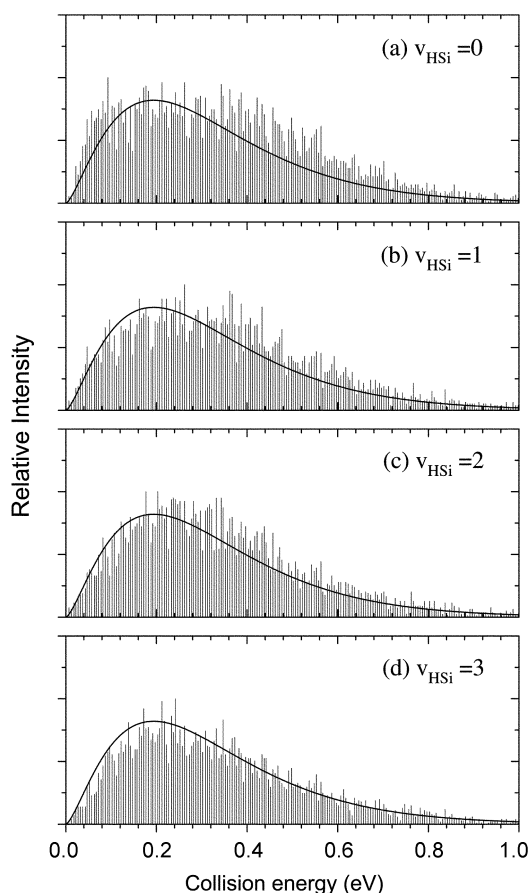


Figure 2. Distributions of collision energies of the reactive collisions for the HBr formation for the initial vibrational state of the adsorbate from $\nu_{\text{HSi}} = 0$ to 3. The solid line is the sampled collision energies.

high energy region of the Maxwell distribution interacts with the surface. For $\nu_{\text{HSi}} = 1$, however, the distribution of collision energies of reactive trajectories follows the Maxwell distribution almost as closely as the total sampled trajectories [see Figure 2(b)]. As shown in Figures 2(c) and (d), the distributions of collision energies of reactive trajectories for $\nu_{\text{HSi}} = 2$ and 3 show the similar distribution as for $\nu_{\text{HSi}} = 1$.

Secondly, we consider the distribution of reaction times for the HBr formation reaction in Figure 3. To determine this time scale, we first confirm the occurrence of a reactive event by following the motion of $\text{HBr}(\text{g})$ for 50 ps. When $\text{HBr}(\text{g})$ does not adsorb again on the surface and is completely away from the influence of surface interactions, we trace the reactive trajectory backward to find the time at which the H to Si separation has reached $r_{\text{HSi,e}} + 5.0 \text{ \AA}$, where $r_{\text{HSi,e}}$ is the equilibrium distance of the H-Si bond (1.514 \AA). We define the period from the start of collision to the time at which the HSi distance reaches $(r_{\text{HSi,e}} + 5.0)$ as the reaction time t_R .⁹ The reaction times for the HSi vibration in the ground state, that is, $\nu_{\text{HSi}} = 0$ are much longer than those for the excited states [see Figures 3(a)-(d)]. Thus, Si-H vibration in the ground state receives more energy from the incident atom and retains it long enough for the bond to dissociate [see Figures 2(a) and 3(a)]. Therefore, the reaction

Table 1. Potential and Spectroscopic Constants

interaction (i)	H-Br	H-Si	Br-surface
$D_{0,i}^0 (\text{eV})^a$	3.458	3.500	0.245
$\omega_i (\text{cm}^{-1})^b$	2649	2093	
$d_i (\text{\AA})^c$	1.414	1.514	4.000
$a_i (\text{\AA})^d$	0.265	0.334	0.350

^a $D_i = D_{0,i}^0 + 1/2h\omega_i$ (ref. 19 for H-Br; refs. 20 and 21 for H-Si; ref. 23 for Br-Si). ^bRef. 19 for H-Br; refs. 4 and 22 for H-Si. Here the HSi value 2093 cm^{-1} is the z-direction vibrational frequency $\omega_{\text{HSi,z}}$. For the x and y directions, the vibrational frequencies are $\omega_{\text{HSi,x}} = \omega_{\text{HSi,y}} = 645 \text{ cm}^{-1}$. ^cRef. 19 for H-Br; ref. 22 for H-Si; ref. 24 for Br-Si. ^d $a_i = (D_i/2\mu_i)^{1/2}(1/\omega_i)$.

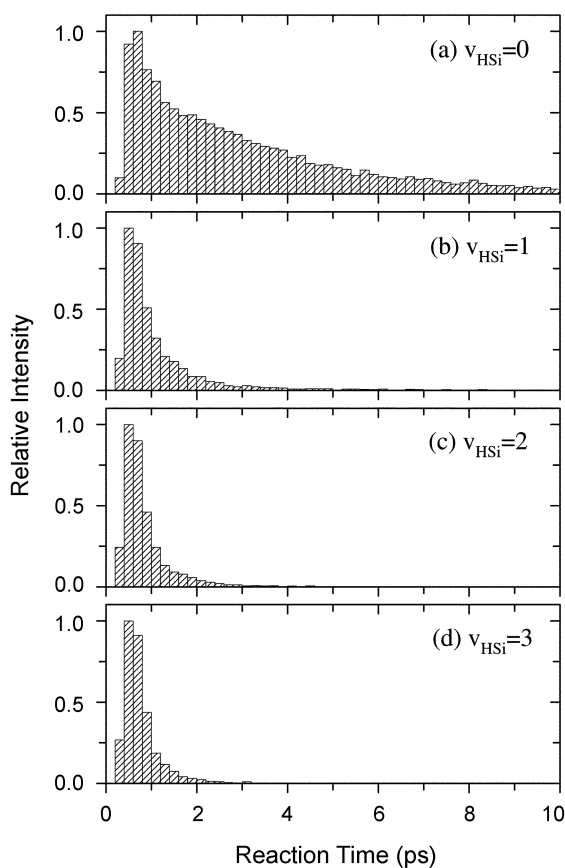


Figure 3. Reaction time distributions for the HBr formation reaction depending on the initial vibrational state of the adsorbate from $\nu_{\text{HSi}} = 0$ to 3.

probability in the ground state is significantly high, even though the reaction is endothermic. As mentioned above, the distribution of collision energies of reactive trajectories for $\nu_{\text{HSi}} = 1$ follows the Maxwell distribution as closely as the sampled trajectories. Furthermore, the reaction time for $\nu_{\text{HSi}} = 1$ is significantly shorter than that for $\nu_{\text{HSi}} = 0$. Thus, even though the reaction for $\nu_{\text{HSi}} = 1$ is exothermic, the reaction probability is as close as that for $\nu_{\text{HSi}} = 0$. The same is true for $\nu_{\text{HSi}} = 2$ and 3 too. On the other hand, as shown in Figures 3(b)-(d), as the vibrational state of the adsorbed hydrogen atom increases, the reaction time decreases slightly. As the vibrational state of the adsorbed hydrogen rises, the reaction exothermicity increases. Thus, the reaction time, that is, the time to take enough energy for the adsorbed hydrogen atoms to dissociate is shorter. As shown in Figure 3(b), almost all events for $\nu_{\text{HSi}} = 1$ are completed within 10 ps. Furthermore, examination of the collision trajectories reveals that about three quarters of the total reactive trajectories leading to the HBr formation occur on direct-mode collision. Remaining reactive events occur on multiple impact collision.^{6,9} As the vibrational state of the adsorbed hydrogen atom increases, however, the fraction of multiple impact collision decreases because the reaction exothermicity increases.

To discuss the reaction time shown in Figure 3 in detail, we select a trajectory which is representative of direct-mode

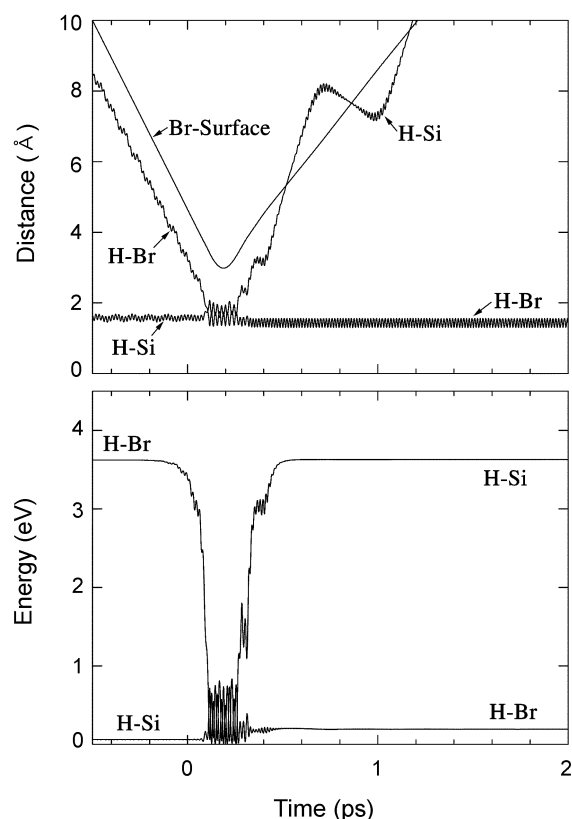


Figure 4. Dynamics of the representative trajectory for a direct-mode collision in HBr formation reaction. (a) Time evolution of the Br to surface, H-Si, and H-Br distances. (b) Time evolution of the Br to H interaction energy and the H-Si vibrational energy.

collisions of HBr formation reaction and plot the time evolution of its gas atom-surface distance Z (*i.e.*, the collision trajectory), adatom-surface distance r_{HSi} , and the Br to H distance r_{HBr} in Figure 4(a). The time evolution of HBr and HSi vibrational energies is shown in Figure 4(b). The oscillation of the outgoing r_{HSi} is due to the rotation of HBr. It is not possible to determine when the reaction begins from the time evolution of Z shown in Figure 4(a). However, the time evolution of the H-Si or H-Br interactions displayed in Figure 4(b) clearly shows the weakening of the H-Si bond or the formation of the H-Br bond. Near $t = 0$, when the Br to surface distance is 6 \AA , the H to Br interaction energy begins to decrease, indicating the start of reaction. (In the numerical procedure, all reactive collisions begin at a time close to 0.) The Br atom reaches the turning point at $t = 0.19 \text{ ps}$, and then the product HBr recedes to 5 \AA from the surface at $t = +0.50 \text{ ps}$ [see Figure 4(a)]. Thus, we can say that the collision begins (or ends) when the incident atom (or the product molecule) reaches a distance of $5\text{--}6 \text{ \AA}$ from the surface. Our choice of 5.0 \AA for H-Si displacement as the occurrence of a reactive event and the above-defined reaction time scale are based on this time evolution. Therefore, in the present representative collision, the reaction time becomes 0.31 ps . Beyond $t = +0.5 \text{ ps}$, the HBr vibration stabilizes to a constant value of 0.194 eV [see Figure 4(b)].

In Figure 5, we show the time evolution of a representative trajectory of multiple impact collisions. These events may be considered as hot-atom mechanism.⁹ The Br-to-surface interaction begins near $t = 0$, and the incident Br atom suffers the first impact with the surface near $t = +0.3$ ps. At this time, the Br atom comes in close range of the adatom causing a significant disturbance in the H-Si interaction. As shown in Figure 5(a), however, the Br atom does not pick up the adsorbed H atom and fly away with it in this first impact. The Br atom interacts with the adatom to form a weak H-Br bond and the interaction is not strong enough to break the H-Si bond. This is a barely trapped trajectory, thus forming a loosely bound complex on the surface, Br-H-Si. The Br atom rebounds several times until it accumulates enough energy to break the H-Si bond, spending a relatively long time above the surface. Thus, the reaction time becomes longer than the direct-mode collision. Furthermore, as the reaction exothermicity becomes smaller or negative, these multiple impact collisions occur more often [see Figure 3]. After completing several oscillations, the Br atom is attracted back to the surface for final impact near $t = +2.7$ ps, at which time Br abstracts H and move away from the surface. The receding molecule reaches a distance of 5 Å at $t = +3.8$ ps. Thus, in the present representative collision, the reaction time becomes 3.5 ps and the product molecule deposits 0.102 eV in its vibrational motion [see Figure 5(b)].

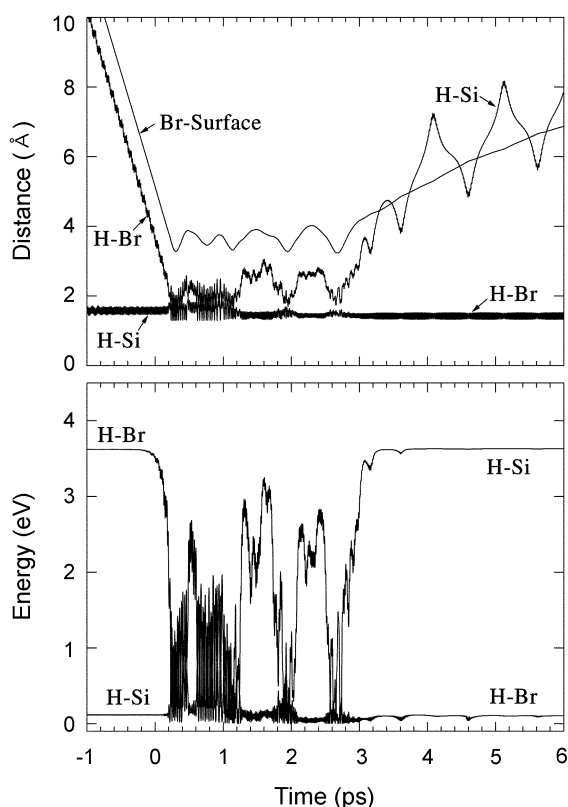


Figure 5. Dynamics of the representative trajectory for a multiple impact collision in HBr formation reaction. (a) Time evolution of the Br to surface, H-Si, and H-Br distances. (b) Time evolution of the Br to H interaction energy and the H-Si vibrational energy.

In Figure 6 we show the dependence of the opacity function $P(b)$ on the impact parameter for the HBr formation. This b -dependence provides useful information about the region where HBr formation occurs. For the adatom-surface vibration initially in the ground state, the HBr formation occurs toward small b collisions. The probability $P(b)$ is 0.25 in $b \cong 0$ collisions and then rises to a maximum value near $b = 0.5$ and then decreases to zero with increasing b [see Figure 6(a)]. This indicates that the HBr formation occurs mostly in the neighborhood of the adatom site. In their quasi-classical study of Eley-Rideal recombinative desorption of H_2 from Cu(111), Persson and Jackson²⁷ also found that the dominant contribution to the cross section comes from a narrow range of impact parameters. When the vibrational state $v_{\text{HSi}} = 1$, the maximum of the opacity function shifts generally toward larger b . The normal component of the incident energy is $E \cos^2 \theta_{\text{inc}}$. Therefore, when the impact parameter is larger, the normal component of the incident energy is small, and the available energy for the H desorption becomes smaller. For the excited HSi vibrational states, however, this loss of energy is more than compensated by the exothermicity of the reaction, and the large b collisions can lead to the HBr formation reaction. On the other hand, for the $v_{\text{HSi}} = 0$ case, in which the reaction is endothermic, the large b collisions can not lead to the reactive HBr formation.

The total reaction cross section calculated using the impact parameter-dependent probability function $P(b)$, the opacity function, from the expression $2\pi \int_0^{b_{\text{max}}} P(b) b db$ is 2.53 \AA^2 for the HBr formation reaction when $v_{\text{HSi}} = 0$.⁹ It

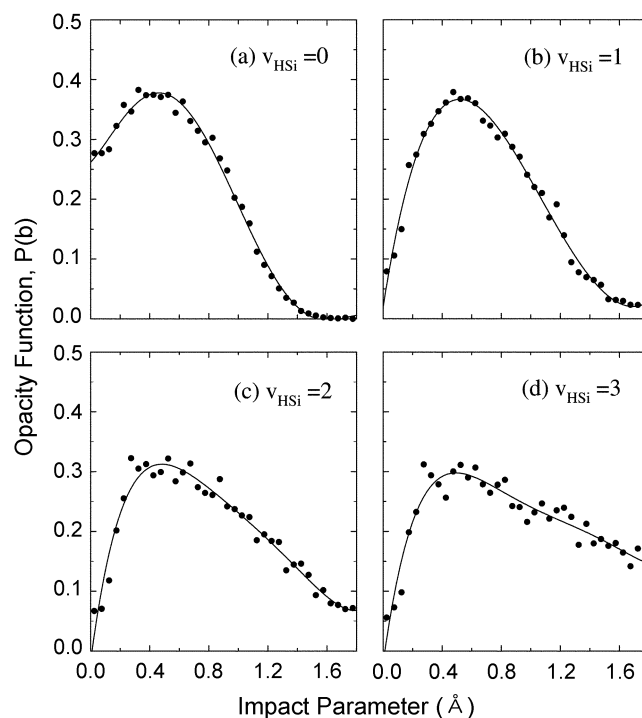


Figure 6. Dependences of the HBr formation on the impact parameter for the initial vibrational state of the adsorbate from $v_{\text{HSi}} = 0$ to 3.

rises to 3.06, 3.56, and 4.34 Å² when ν_{HSi} is increased to 1, 2, and 3, respectively. This is because, as mentioned above, the reaction events shift toward the high impact parameter side when the Si-H vibrational state is increased, even though the reaction probability does not significantly increase. This is very similar to the reaction $\text{O}(\text{g}) + \text{H}(\text{ad})/\text{Si} \rightarrow \text{OH}(\text{g}) + \text{Si}$, in which it is 2.54 Å² for $\nu_{\text{HSi}} = 1$ but rises to 4.45 Å² when ν_{HSi} is increased to 3.²⁶

Product Energy Distribution. The energy available for HBr and the surface in $\text{Br}(\text{g}) + \text{H}(\text{ad})/\text{Si}$ is $(\Delta D_0^0 + E_{\text{HSi}}^0 + E)$, where E_{HSi}^0 is the initial energy of the adatom-surface vibration and E is the bromine atom kinetic energy. The quantity ΔD_0^0 is the difference between the HSi dissociation energy and HBr dissociation energy.

In Table 2, we summarize the ensemble-averaged values of energies deposited in the vibrational, rotational and translational motions of HBr as well as that propagated into the solid for $\nu_{\text{HSi}} = 0, 1, 2$ and 3 at the thermal conditions of $(T_{\text{g}}, T_{\text{s}}) = (1500, 300 \text{ K})$. For $\nu_{\text{HSi}} = 1$, the energies deposited in the vibrational, rotational and translational motions of HBr are $\langle E_{\text{vib}} \rangle = 0.206$, $\langle E_{\text{rot}} \rangle = 0.037$ and $\langle E_{\text{trans}} \rangle = 0.191$ eV. The amount of energy propagated into the solid $\langle E_{\text{s}} \rangle$ is 0.011 eV. Thus, the gas-phase product HBr carries away the majority of the reaction exothermicity. In particular, nearly 90% of the reaction energy is deposited in the vibrational and translational motions. This type of product energy distribution with a major portion depositing in translation and vibration is characteristic of an ER mechanism.^{5,28} The ensemble-averaged energy transfer to the silicon surface $\langle E_{\text{s}} \rangle$ is 0.011 eV, that is, a part of the reaction energy is propagated into the bulk solid phase. It is interesting to note that $\langle E_{\text{s}} \rangle$ for the vibrational state $\nu_{\text{HSi}} = 0$ at the same thermal conditions is -0.027 eV, which means that the desorbing HBr molecule takes away energy from the surface because the reaction is endothermic. Increasing the initial vibrational state of the adsorbate vibration from $\nu_{\text{HSi}} = 1$ to 2 and 3 changes the surface energy $\langle E_{\text{s}} \rangle$ only slightly. However, there is a large increase in the desorbing HBr energy with increasing ν_{HSi} , equally in the vibrational, translational and rotational motion. This result is different from that for the related system of $\text{O}(\text{g})$ interacting with $\text{H}(\text{D})(\text{ad})/\text{Si}$, where the OH translational energy, as well as the surface energy change only slightly whereas a large increase in the vibrational energy occurs with increasing initial excitation of the HSi vibration.²⁶ Ree *et al.* suggested that for the system $\text{O}(\text{g}) + \text{H}(\text{ad})/\text{Si}$ the additional energy available from initial H-Si vibrational excitation preferentially

flows toward the O...H bond in the short-lived O...H-Si complex and eventually deposits in the vibration.²⁶ In the present system, however, since Br is much more heavier than O, the energy flow from the H-Si bond to the Br...H bond in the system $\text{Br}(\text{g}) + \text{H}(\text{ad})/\text{Si}$ is less than that in the system $\text{O}(\text{g}) + \text{H}(\text{ad})/\text{Si}$. Therefore, the additional energy is equally distributed to three motions, not preferentially to the Br-H vibrational motion.

When the initial vibrational state of the adsorbate is raised from $\nu_{\text{HSi}} = 0$ to 1, corresponding to the increase of initial vibrational energy by 0.256 eV, the ensemble-averaged energy deposited in the HBr vibration increases from $\langle E_{\text{vib}} \rangle = 0.133$ eV to 0.206 eV, an increase of 0.073 eV, whereas $\langle E_{\text{trans}} \rangle$ increases from 0.091 to 0.191, an increase of 0.100 eV. That is, increase in $\langle E_{\text{trans}} \rangle$ is more than that in $\langle E_{\text{vib}} \rangle$. This is expected from Figure 3(a) and 3(b). In Figure 3(a), the reaction time is significantly long and most reaction events occur by multiple impacts. In this case, the Br atom stays on the surface for a long time and the product HBr recedes from the surface with a smaller kinetic energy. In Figure 3(b), however, the reaction time is significantly shorter and in this case receding HBr is accelerated with higher kinetic energy. A similar increase is seen when ν_{HSi} rises from 1 to 2 and 2 to 3. There are other sources of energy, which can contribute to the newly formed HBr bond, but the main contributor to the vibrational energy of HBr is the H-Si bond. So, the V→V energy transfer pathway becomes more important when ν_{HSi} rises. Thus, nearly half of the energy initially deposited in the HSi vibration transfers to the nascent HBr vibration. This efficient flow of energy occurs at close range during Br(g)-to-H(ad)/Si interaction. At this range where the incident bromine atom moves along the reaction coordinate, it becomes loosely bound to the adatom forming a short-lived collision complex ($\text{Br}\cdots\text{H-Si}$), in which "quasi-intramolecular" VV coupling occurs. This coupling promotes an asymmetric stretching vibration of the three-atom configuration causing the Br...H bond to strengthen as the H-Si bond weakens in a concerted mechanism. On the other hand, we note that for the $\nu_{\text{HSi}} = 0$ case the incident atom carries a significant amount of the collision energy and its transfer to the nascent vibration is efficient, *i.e.*, a collision-induced T → V energy transfer process is efficient in this endothermic reaction.

The vibrational energy-to-impact parameter relation for all HBr forming events plotted in Figures 7(a)-(d) shows a gradual increase of the vibrational energy of HBr as the initial vibrational excitation of HSi increases. Reactive events become scattered to higher vibrational energies and wider impact parameter ranges as ν_{HSi} increases. The scattering to larger b collisions leads to HBr rotation sharing more amount of the reaction energy. We can recast the results presented in Figures 5(a)-(d) in the vibrational population as shown in Figure 7(e)-(h), where the intensity mimics the quantum vibrational distribution formulated by use of a binning procedure of assigning quantum number ν_{HBr} corresponding to $\nu_{\text{HBr}} = \text{int}[E_{\text{vib}}/E_{\text{vib}}(\nu_{\text{HBr}})]$. Here E_{vib} is the vibrational energy calculated in the present study and

Table 2. Distribution of the Reaction Exothermicity at 1500 and 300 K^a

ν_{HSi}	$\langle E_{\text{vib}} \rangle$	$\langle E_{\text{rot}} \rangle$	$\langle E_{\text{trans}} \rangle$	$\langle E_{\text{s}} \rangle$
0 ^b	0.133	0.020	0.091	-0.027
1	0.206	0.037	0.191	0.011
2	0.314	0.073	0.252	0.008
3	0.467	0.119	0.291	0.006

^aAll energies are in eV. ^bFrom Ref. 9.

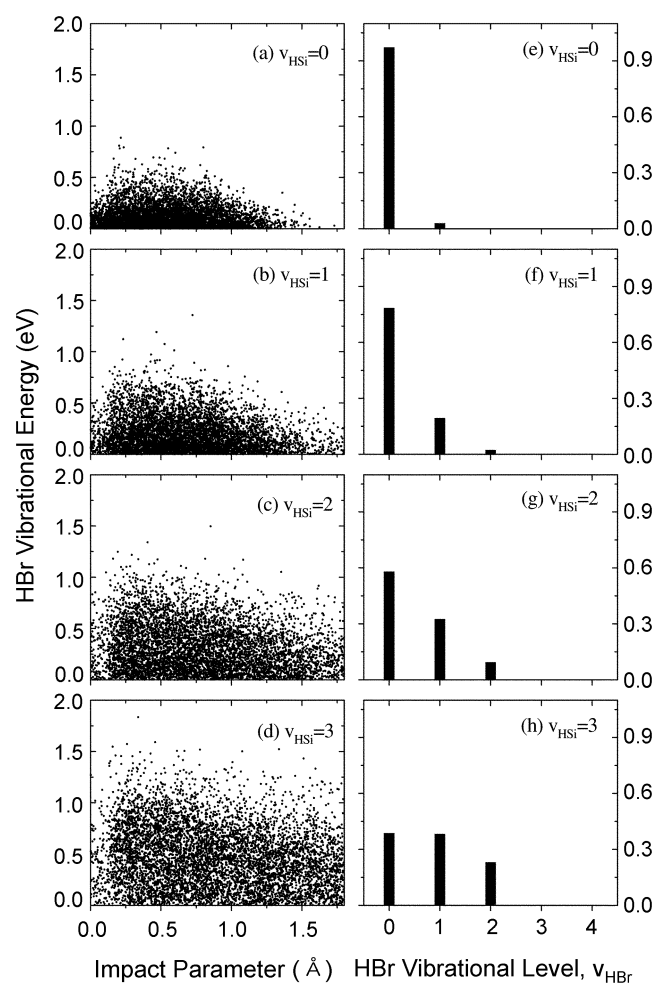


Figure 7. Distributions of the newly formed HBr vibrational energy as a function of the impact parameter for the initial vibrational states of the adsorbate from $\nu_{\text{HSi}} = 0$ to 3; the left four graphs (a–d). HBr vibrational population distribution; the right four graphs (e–h).

$E_{\text{vib}}(\nu_{\text{HBr}})$ is the vibrational energy determined from the eigenvalue expression $E_{\text{vib}}(\nu_{\text{HBr}})/hc = \omega_e(\nu_{\text{HBr}}+1/2) - \omega_e x_e(\nu_{\text{HBr}}+1/2)^2 + \omega_e y_e(\nu_{\text{HBr}}+1/2)^3$ with $\omega_e = 2648.98 \text{ cm}^{-1}$, $\omega_e x_e = 45.217 \text{ cm}^{-1}$, $\omega_e y_e = -0.003 \text{ cm}^{-1}$. As shown in Figure 7(e), for the initial vibrational energy of HSi corresponding to $\nu_{\text{HSi}} = 0$, the binning procedure yields the relative HBr vibrational intensities of 0.971, 0.028, and 1.62×10^{-4} for $\nu_{\text{HBr}} = 0, 1$, and 2, respectively. For the initial vibrational energy of HSi corresponding to $\nu_{\text{HSi}} = 1$, the intensity of the vibrational population for the $\nu_{\text{HBr}} = 1$ level is as large as 0.194 compared with 0.783 for $\nu_{\text{HBr}} = 0$, which represents the vibrational population seriously deviating from the prediction of the Boltzmann distribution. At gas temperature 1500 K, the Boltzmann distribution gives the fractions $f(\nu_{\text{HBr}} = 0) = 1 - e^{-h\nu/kT} = e^{-hc\nu/kT} = 0.921$ and $f(\nu_{\text{HBr}} = 1) = (1 - e^{-h\nu/kT})e^{-h\nu/kT} = (1 - e^{-hc\nu/kT})e^{-hc\nu/kT} = 0.073$, so the ratio $f(\nu_{\text{HBr}} = 1)/f(\nu_{\text{HBr}} = 0)$ is only 0.079. Therefore, the present result shown in Figure 7(f) giving $f(\nu_{\text{HBr}} = 1)/f(\nu_{\text{HBr}} = 0) = 0.247$ seriously deviates from the prediction of the Boltzmann distribution. The deviation becomes even larger when ν_{HSi} is

Table 3. Dependence of the Product Energy Distribution on the Surface Temperature

(a) $\nu_{\text{HSi}} = 0$				
T_s (K)	$\langle E_{\text{vib}} \rangle$	$\langle E_{\text{rot}} \rangle$	$\langle E_{\text{trans}} \rangle$	$\langle E_s \rangle$
0	0.130	0.017	0.087	0.056
300	0.133	0.020	0.091	-0.027
600	0.136	0.023	0.099	-0.070
(b) $\nu_{\text{HSi}} = 3$				
T_s (K)	$\langle E_{\text{vib}} \rangle$	$\langle E_{\text{rot}} \rangle$	$\langle E_{\text{trans}} \rangle$	$\langle E_s \rangle$
0	0.444	0.104	0.302	0.064
300	0.467	0.119	0.291	0.006
600	0.497	0.120	0.286	-0.079

raised. For example, for $\nu_{\text{HSi}} = 2$ shown in Figure 7(g), the population intensity of $\nu_{\text{HBr}} = 1$ is now 0.325 compared with 0.580 for $\nu_{\text{HBr}} = 0$. For $\nu_{\text{HSi}} = 3$, the intensities are 0.386, 0.382, 0.230 and 0.002 for $\nu_{\text{HBr}} = 0, 1, 2$ and 3, respectively [see Figure 7(h)]. The high vibrational excitation of HBr reported here is characteristic of the ER mechanism.

Now, we briefly comment on the dependence of reaction probabilities and product energy distributions on surface temperature; see Table 3. Here the gas temperature is fixed at 1500 K as in Table 2 and the values for $T_s = 300$ K are reproduced from Table 2. For $\nu_{\text{HSi}} = 0$, reaction probabilities are 0.267, 0.200 and 0.185 for $T_s = 0, 300$ and 600 K, respectively. This shows a significant negative temperature dependence. For $\nu_{\text{HSi}} = 3$, however, those are 0.225, 0.221 and 0.223 for $T_s = 0, 300$ and 600 K, respectively, showing no temperature dependence. The principal qualitative feature of product energy distributions is the weak temperature dependence for all initial vibrational energies of HSi considered. That is, the variation of surface temperature is of little consequence in determining the energies of gas-phase product HBr. However, the energy pattern propagated into the bulk surface is very peculiar. For $\nu_{\text{HSi}} = 0$ case, $\langle E_s \rangle$ is 0.056 eV at $T_s = 0$ K, that is, the energy is propagated into the bulk surface. However, at $T_s = 300$ and 600 K, $\langle E_s \rangle$'s are -0.027 eV and -0.070 eV, respectively, which means that the energy is taken away from the solid surface. Furthermore, the higher the surface temperature is, the more the energy is taken away from the solid surface. The trend is generally similar for $\nu_{\text{HSi}} = 3$ case too.

Concluding Comments

We have studied the interaction of gas phase atomic bromine with a highly covered chemisorbed hydrogen atoms on a silicon surface with particular emphasis on the disposal of the reaction exothermicity for a range of initial excitation of the adatom-surface vibration. At gas temperature 1500 K and surface temperature 300 K, the HBr formation reaction probability is significantly high for all the excited H(ad)-Si(s) vibrations considered. For $\nu_{\text{HSi}} = 0$, less than half of reactive events occur on a subpicosecond time scale through direct-mode collisions, while remaining reactive events

occur on reaction time scale longer than one picosecond through hot-atom collisions, which may be regarded as precursor type mechanism. When the HSi vibrational state rises, however, the HBr formation reactive events occur mostly through the direct-mode collision. When $v_{\text{HSi}} = 0$, the product HBr is ejected from the surface on a significantly long time scale in a small impact-parameter collision. As v_{HSi} increases, however, reactive events become scattered to wider impact parameter ranges. A major portion of the reaction exothermicity deposits in the vibrational and translational motions of HBr, while a much smaller amount transfers to the rotational motion. In particular, when $v_{\text{HSi}} = 0$, the amount of energy propagated into the surface is negative, but the latter becomes positive as v_{HSi} increases. The dependence of energy distributions on surface temperature is found to be weak in the range of 0-600 K. The energy initially stored in the adatom-surface vibration equally transfers to the vibrational, translational and rotational motions of HBr. Vibrational population for $v_{\text{HSi}} = 0$ follows the Boltzmann distribution, but it seriously deviates from the prediction of the Boltzmann distribution when the initial vibrational energy of the adsorbate increases.

Acknowledgement. This work was financially supported by research fund of Chonnam National University in 2003. Computational time was supported by "the 5th Super-computing Application Support Program" of the KISTI (Korea Institute of Science and Technology Information).

References

1. Shustorovich, E. *Surf. Sci. Rep.* **1986**, 6, 1.
2. Christmann, K. *Surf. Sci. Rep.* **1988**, 9, 1.
3. Koleske, D. D.; Gates, S. M.; Jackson, B. *J. Chem. Phys.* **1994**, 101, 3301.
4. Kratzer, P. *J. Chem. Phys.* **1997**, 106, 6752.
5. Buntin, S. A. *J. Chem. Phys.* **1998**, 108, 1601.
6. Ree, J.; Shin, H. K. *J. Chem. Phys.* **1999**, 111, 10261.
7. Ree, J.; Kim, Y. H.; Shin, H. K. *Chem. Phys. Lett.* **2002**, 353, 368.
8. *CRC Handbook of Chemistry and Physics*, 64th Ed.; Weast, R. C., Ed.; CRC Press: 1983; pp F176-F181.
9. Ree, J.; Chang, K. S.; Moon, K. H.; Kim, Y. H. *Bull. Korean Chem. Soc.* **2001**, 22, 889.
10. Kim, Y. H.; Ree, J.; Shin, H. K. *J. Chem. Phys.* **1998**, 108, 9821.
11. Adelman, S. A. *J. Chem. Phys.* **1979**, 71, 4471.
12. Tully, J. C. *J. Chem. Phys.* **1980**, 73, 1975.
13. Kim, W. K.; Ree, J.; Shin, H. K. *J. Phys. Chem. A* **1999**, 103, 411.
14. Radeke, M. R.; Carter, E. A. *Phys. Rev. B* **1996**, 54, 11803.
15. Koleske, D. D.; Gates, S. M. *J. Chem. Phys.* **1993**, 99, 8218.
16. McEllistren, M.; Buehler, E. J.; Itchkawitz, B. S.; Boland, J. J. *J. Chem. Phys.* **1998**, 108, 7384.
17. *American Institute of Physics Handbook*, 3rd ed.; Gray, D. E., Ed.; McGraw-Hill: New York, 1972; pp 4-116.
18. Lim, S. H.; Ree, J.; Kim, Y. H. *Bull. Korean Chem. Soc.* **1999**, 20, 1136.
19. Huber, K. P.; Herzberg, G. *Constants of Diatomic Molecules*; Van Nostrand Reinhold: 1979.
20. Van de Walle, C. G.; Street, R. A. *Phys. Rev. B* **1995**, 51, 10615.
21. Kratzer, P.; Hammer, B.; Norskov, J. K. *Phys. Rev. B* **1995**, 51, 13432.
22. Tully, J. C.; Chabal, Y. J.; Raghavachari, K.; Bowman, J. M.; Lucchese, R. R. *Phys. Rev. B* **1985**, 31, 1184.
23. Vidali, G.; Ihm, G.; Kim, H.-Y.; Cole, M. W. *Surf. Sci. Rep.* **1991**, 12, 133.
24. Huheey, J. E.; Keeter, E. A.; Keiter, R. L. *Inorganic Chemistry*; Harper Collins College Publishers: 1993.
25. Struve, W. S.; Krenos, J. R.; McFadden, D. L.; Herschbach, D. R. *J. Chem. Phys.* **1975**, 62, 404.
26. Ree, J.; Kim, Y. H.; Shin, H. K. *J. Phys. Chem. A* **2003**, 107, 5101.
27. Persson, M.; Jackson, B. *J. Chem. Phys.* **1995**, 102, 1078.
28. Gross, A. *Surf. Sci. Rep.* **1998**, 32, 291.